

## ANALYSIS AND OPTIMIZATION OF ABSORBING BOUNDARY METHODS FOR ACOUSTIC WAVE MODELLING

Pessolani, R.B.V<sup>a,b</sup>, Matsumoto, R. M.<sup>b</sup>, Kasuga<sup>b</sup>, T.

<sup>a</sup>*Departamento de Eng. Mecânica, Universidade Federal Fluminense,  
R. Passo da Pátria, 156 cep 24230-00 Niterói, Rio de Janeiro Brazil, raul@vm.uff.br*

<sup>b</sup>*LabCFD, Universidade Federal Fluminense  
R. Passo da Pátria, 156 cep 24230-00 Niterói, Rio de Janeiro, Brazil, roger@vm.uff.br*

**Keywords:** Geophysics, Acoustic Wave, Computational Methods, Absorbing Boundary Conditions

**Abstract.** This paper presents numerical simulations obtained via a 10<sup>-4</sup> (10<sup>th</sup> order in space and 4<sup>nd</sup> order in time) staggered-grid finite difference scheme applied to acoustic waves. Our goal is to enhance the classical absorbing boundary methods – namely Absorbing Boundary Condition (ABC), Damping Zone (DZ) and Perfect Matched Layer (PML) – in order to minimize the spurious reflections associated with, improving the quality of the numerical results and reducing its computational effort. ABC, PML and DZ methods are implemented and tested for different coefficients and varying absorbing layers and are also combined. It has been found that both optimizations increase the effectiveness of the absorbing layer, with better absorption efficiencies for the ABC and optimized Cerjan and PML methods. Those methods can reduce significantly the artificial reflections at the boundaries when compared to the conventional attenuation coefficients. Results also show that side effects are very sensitive to the number of grid points used in the absorbing layer, with better results found for larger discretization points.

## 1 INTRODUCTION

The appearance of fast processing computers and the continuous advances in numerical analysis have allowed new developments in acoustic wave modeling. For imaging the subsurface, many articles have been published dealing with numerical simulations of wave propagation using finite difference, finite element and boundary integral methods (Virieux 1986, Marfurt 1984, Schuster 1985, Durran 1999). A typical difficulty that arises when solving numerically such boundary value problems is how to express the radiation condition mathematically at a contour which is only at a finite distance from the energy source (Sommerfeld 1949). The boundary condition should allow travelling disturbances to pass through the contour without generating spurious reflections that propagate back toward the interior, which may eventually override the original emitted seismic signals.

To avoid these side effects, researchers used to enlarge the computational domain, delaying the backward reflections, though increasing the numerical mesh and its computational demand. In the late 70's, nonreflecting boundary condition techniques were introduced aiming to treat such problems. Clayton and Engquist (1977) proposed the Absorbing Boundary Condition (ABC) technique by applying a one-way wave equation in the boundary region, which proved to be efficient for events not at shallow angles on the contour. In the early 80's, Cerjan *et al.* (1985) introduced the Damping Zone (DZ) concept in which a gradual reduction of the wave amplitude is imposed along an absorption layer, without any loss of effectiveness due to shallow angles of wave incidence. More recently, Berenger (1994) proposed the Perfect Matched Layer (PML) method for solving electromagnetic and elastic wave equations. A new matched medium is designed to absorb without reflection the incident waves at any frequency and at any incidence angle.

This article presents numerical simulations obtained via a 10<sup>th</sup> order in space and 4<sup>th</sup> order in time staggered-grid finite difference scheme applied to acoustic waves. Figure 1 exemplifies the wave propagation domain with its absorbing boundary layers. Our main motivation is to reduce the number of grid points at the absorbing boundary layer for the least reflected waves inside the medium. Our goal is to enhance the existing absorbing boundary methods in order to minimize the errors associated with, improving the quality of the numerical results and reducing its computational effort. First, DZ, PML and ABC methods are presented and optimized aiming to reduce wave reflection at the borders, with results shown in terms of the total energy for "infinite" and nonreflecting models for varying absorbing layers. Results are shown in terms of the time sum of squared energy difference between infinite and nonreflecting models for varying absorbing layers.

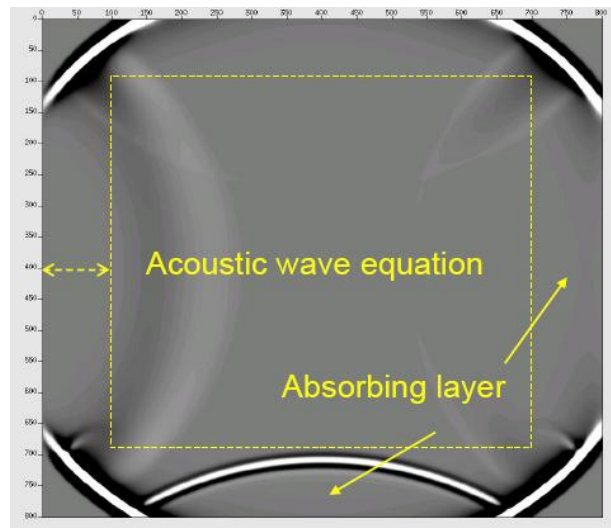


Figure 1. Wave propagation domain with absorbing boundary layers.

## 2 ABC TECHNIQUE

The ABC technique was proposed originally by Clayton and Engquist (1977), transforms the boundary conditions in order to minimize artificial reflections. The new boundary conditions are based on paraxial approximations of the wave equation, which is in fact, an extrapolation of the wave-field inside the domain.

Approximation of the first order is given by:

$$\frac{\partial U}{\partial z} + \frac{1}{v} \frac{\partial U}{\partial t} = 0 \quad (1)$$

Where  $U$  is the wave amplitude and  $v$  is the medium wave speed.

This procedure will be tested, alone and also with other Techniques, described below.

### 2.1 ABC with Liu Technique

In order to minimize the waves that come to the boundary and provide a smooth variation Liu and Sen (2010) proposed to insert a transition area between domain and boundary. They divided the whole domain in three blocks (see figure 2): an inner area (I), the transition (II) and the boundary (III).

The wave field within the inner area is computed using the wave equation, while into the transition area is computed by the wave equation and the one-way equation. The final wave field into the area II is found by applying a weighted average between the two values, given by:

$$U_2 = (1 - w)U_1 + w.U_3 \quad (2)$$

Where  $w$  is the weight factor varying linearly from 1 to zero in ten points of the area II. This procedure provides a smooth variation from area I to area III. In area III, the wave field is calculated by the conventional ABC extrapolation (see Figure 2).

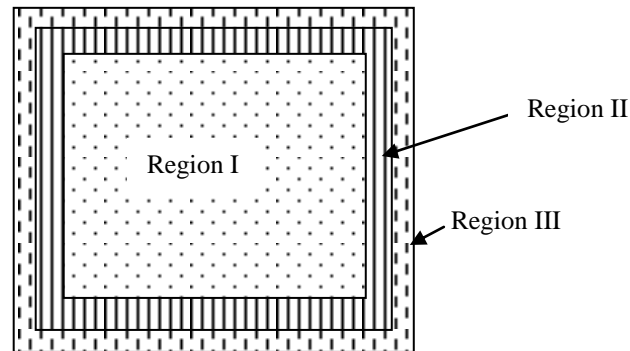


Figure 2 – The three regions of Liu's Method

### 3 PML TECHNIQUE

#### 3.1 Conventional PML

When the disturbances generated by a source reach the limits of the computational domain, reflected waves are spread throughout the medium. To avoid this problem, Berenger (1994) developed the PML technique, in which a new region that surrounds the FDTD domain is defined, where a set of non-physical equations are applied giving a high attenuation of the incident waves.

For acoustics, the 2D linearized continuity and Euler equations take the following form at the PML absorbing layer,

$$p_t + B\alpha p = -B\nabla \cdot \bar{u}, \quad (3)$$

$$\bar{u}_t + B\alpha \bar{u} = -\frac{1}{\rho} \nabla p, \quad (4)$$

where  $\rho$ ,  $p$  and  $\bar{u}$  are, respectively, the medium density and the acoustics pressure and vector velocity, while  $\alpha$  is the attenuation coefficient and  $B (= \rho c^2)$  the medium bulk modulus.  $c$  is the medium wave speed.

Differentiating in time and space equations (3) and (4) and subtracting the resulting expressions gives the PML acoustic equation,

$$p_{tt} + \alpha(1+B)p_t + \alpha^2 Bp = c^2 \nabla^2 p \quad (5)$$

The attenuation coefficient  $\alpha$  varies accordingly to,

$$\alpha(i) = \frac{1}{B\delta t} \ln \left( \frac{1}{r_{PML}} \right) \left[ \frac{x(i)}{x(n_{PML})} \right]^k \quad (6)$$

in which the maximum applied absorption rate  $r_{PML}$  is equal to 1/10 and the exponent  $k=2$ . Therefore  $\alpha$  oscillates from 0 (when  $x$  is at the border of the absorbing layer, thus satisfying the acoustic wave equation) to  $\ln(10)/(B\delta t)$ , where  $\delta t$  is the time step and  $n_{PML}$  the number of PML grid elements. The integer  $i$  represents the grid element such that  $1 \leq i \leq n_{PML}$ .

### 3.2 Optimized PML

In a general form,  $\alpha$  can be rewritten as,

$$\alpha(i) = c_{PML} f[x(i)] \quad (7)$$

Changing the values of  $c_{PML}$  and the function  $f[x(i)]$ , for a fixed  $n_{PML}$ , improves the effectiveness of the absorption, reducing its side effects by increasing the absorption rate and using smoother polynomials at the absorbing layer. Figure 3 shows some of the tested attenuation functions  $f[x(i)]$  for  $n_{PML}=20$

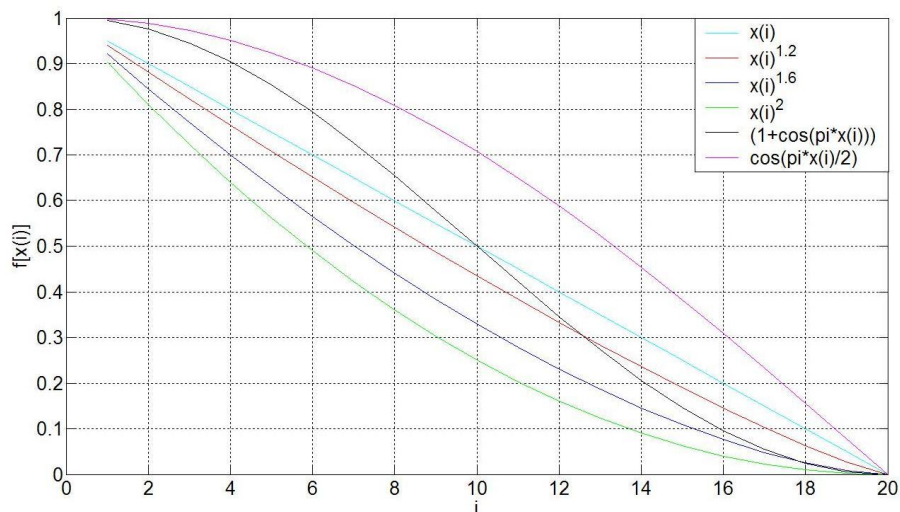


Figure 3. Tested attenuation functions  $f[x(i)]$  for the optimized PML method.

## 4 DZ TECHNIQUES

### 4.1 The Standard Cerjan Method

Conventional Cerjan's (1986) method introduces a damping zone around the domain consisting of  $Na$  points where the wave amplitude is absorbed by the relation,

$$Fac = e^{-(factor*(Na-i))^2} \quad (8)$$

The coefficient  $factor$  is 0,015 for  $Na$  Boundary Layer points in the damping layer and  $i$  varies from 1 to  $Na$ . The factor remains constant through various the numbers of points on the Boundary Layer.

The wave amplitude gradually diminishes, but at the end of the process a small amount of energy is reflected. Though being small, the energy reflection cannot be accepted for more accurate analysis. To minimize the reflected energy, a common procedure is to increase the number of points in the damping layer. At first, the reflected energy diminishes, but from a certain number of points, it tends to remain constant. A procedure to minimize the energy reflected was then developed to try to diminish the error.

### 4.2 Optimized DZ Technique

In order to try to improve the conventional Cerjan's Method, the coefficients factors were

calculated varying the number of points from 20 to 100 on the boundary layer and computing the energy reflection by the square amplitude difference at each time step, between the model with the infinite domain and the order with the artificial boundary. The factors computed are shown in figure 4.

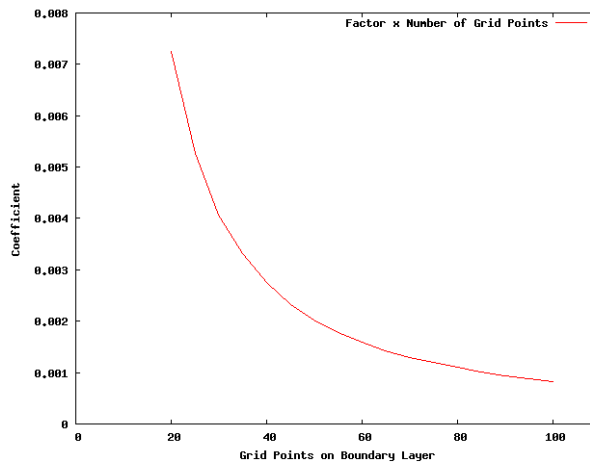


Figure 4: The Coefficient Factor of the Optimized Cerjan Method and the number of boundary layer points.

Figure 5 shows the amount of energy reflection and the number of boundary points. It shows a comparison between the original Cerjan’s method and its optimization. It can be seen that the original Cerjan curve is constant after 25 grid points on the Boundary Layer, while on the Optimized one, the error decrease with the number of grid points on the boundary layer. The main goal is to develop a method that minimize the error and do not increase the computational effort.

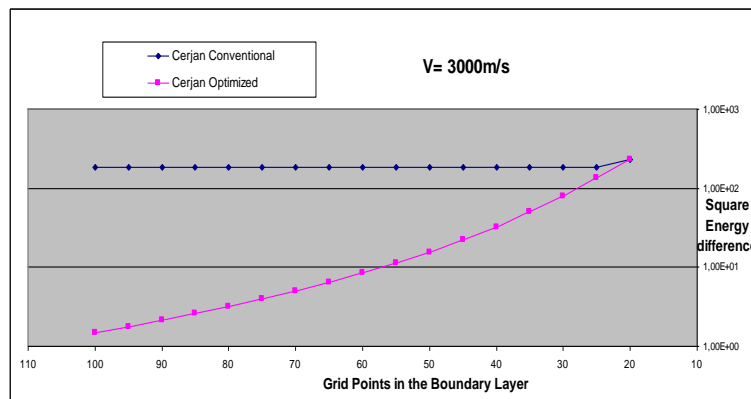


Figure 5 Comparison between Conventional Cerjan and Optimized Cerjan method.

A second step of optimization was the coupling of a factor that reduces the propagation velocity. It was verified that Cerjan factor works better in low velocities. This way, wave equation is:

$$\frac{\partial^2 U}{\partial t^2} = (FRv.C)^2 * \left( \frac{\partial^2 U}{\partial x^2} + \frac{\partial^2 U}{\partial y^2} \right) \tag{9}$$

The equation factor follows a quadratic form:

$$FRv = \frac{(1 - Fv)}{Na^2} x^2 - 2 \frac{(1 - Fv)}{Na} x + 1 \quad (10)$$

Where  $FRv$  vary from 1.0 (when  $x=Na$ ) to  $Fv$  (when  $x=1$ ). This factor enables a reduction of the wave energy reflection in almost 60% compared to Standard Cerjan for boundary layers until 50 points, that is shown in Figure 6.

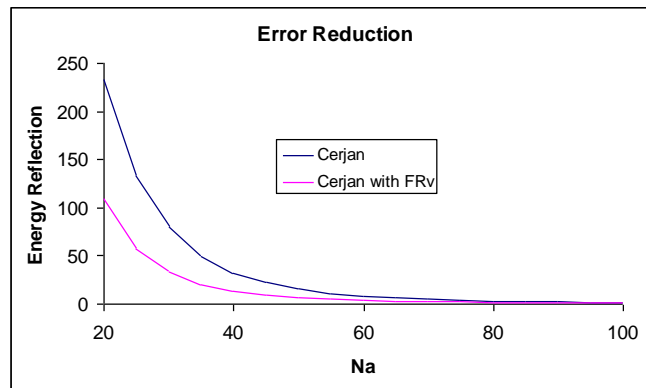


Figure 6 – Wave energy reflection using the velocity reduction factor

## 5 METHODOLOGY

The effectiveness of three different algorithms for wave absorption in the boundary layer was compared. For all algorithms, absorption layers with different thickness were tested. At time  $t=0$ , a Ricker type source is generated at the center of the model and propagated through a finite difference method.

As an energy measure, the square of the amplitude over the whole domain was taken to evaluate the effectiveness of each absorption boundary,

$$E_{Effectiveness} = \sum (U)^2 \quad (11)$$

The model used was a 2D constant velocity (3000 m/s) grid. As shown in Figure 1, the region without the absorption layer (Region 1) has 601x601 grid points. Around this region, a boundary layer was created with thickness varying from 20 to 150 grid points. The wave absorption algorithms were applied on these boundary layers. The finite differences operator used is a second order in time and 10th order in space operator. To avoid instability and divergence problems with the numerical method, grid spacing used was 5 meters and the time step 0,0002 s. Distance between source and receiver was 294 grid points or 1470 m.

## 6 RESULTS

### 6.1 PML Results

Figure 7 compares the effectiveness of wave absorption for the original (PML2-10:  $k=2$ ,  $r_{PML}=1/10$ ) and optimized PML methods (PML5-10:  $k=5$ ,  $r_{PML}=1/10$ ; PML2-1.1:  $k=2$ ,  $r_{PML}=9/10$ ; PML5-1.1:  $k=5$ ,  $r_{PML}=9/10$ ; PML7-10:  $k=7$ ,  $r_{PML}=1/10$ ) with varying absorbing layers. Results show that, for a small number of PML grid elements ( $n_{PML}=25, 50$ ), the application of larger maximum absorption rates ( $r_{PML}=9/10$ ) proves to be more efficient to absorb incident waves, reducing significantly wave reflections at the border.

On the other hand, for larger PML layers ( $n_{PML}=75, 100, 150$ ), a conjugated use of maximum absorption rates ( $r_{PML}=9/10$ ) and higher order polynomials ( $k=5, 7$ ) improve the effectiveness of the absorbing layer. In fact, figure 8 illustrates that the proposed optimized PML models are more effective than the original's Cerjan and PML methods.

As explained in section 2.2, further investigations reveal that better absorption rates can be found for certain values of  $c_{PML}$  and functions  $f[x(i)]$ . Figure 9 shows that a quadratic function for the attenuation function  $f[x(i)]$  with  $c_{PML}=3,55 \times 10^{-8}$  gives the minimum reflection for  $n_{PML}=20$ , which represents less than 0,5% of the total incident wave energy. Other functions were also tested which proved to be more efficient absorbers when compared to the original PML method.

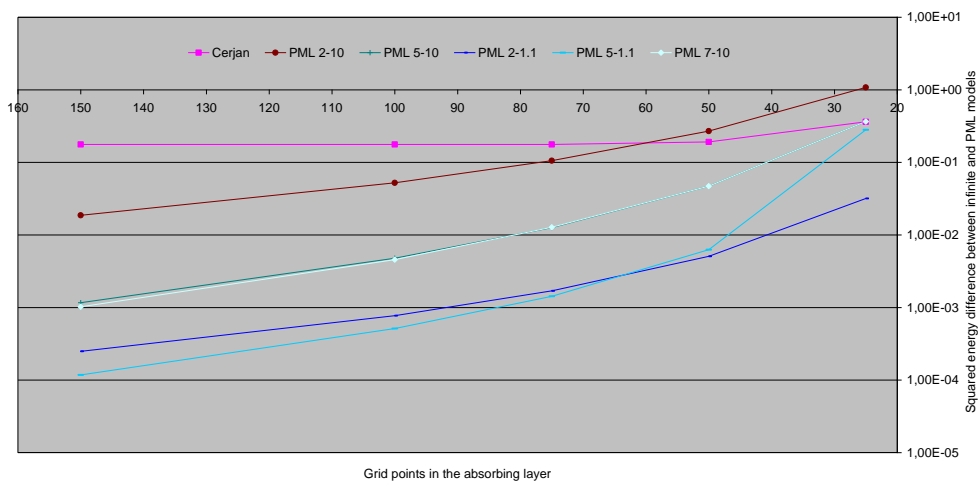


Figure 7. Time sum of squared energy difference between “infinite” and nonreflecting boundary methods for varying absorbing layers.

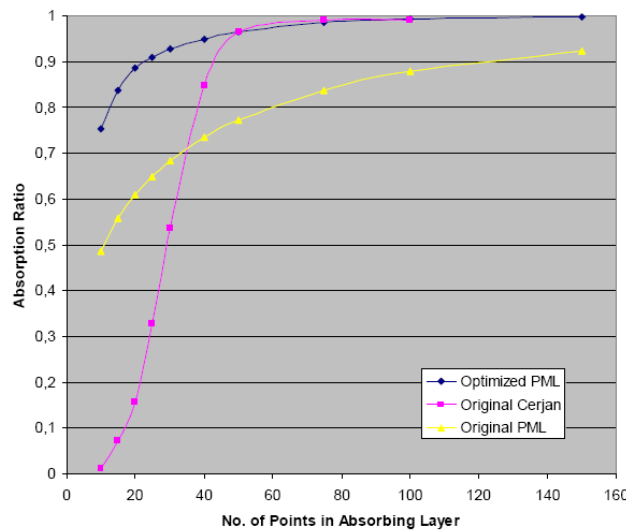


Figure 8. Energy absorption ratio between infinite and nonreflecting boundary methods for varying absorbing layers.

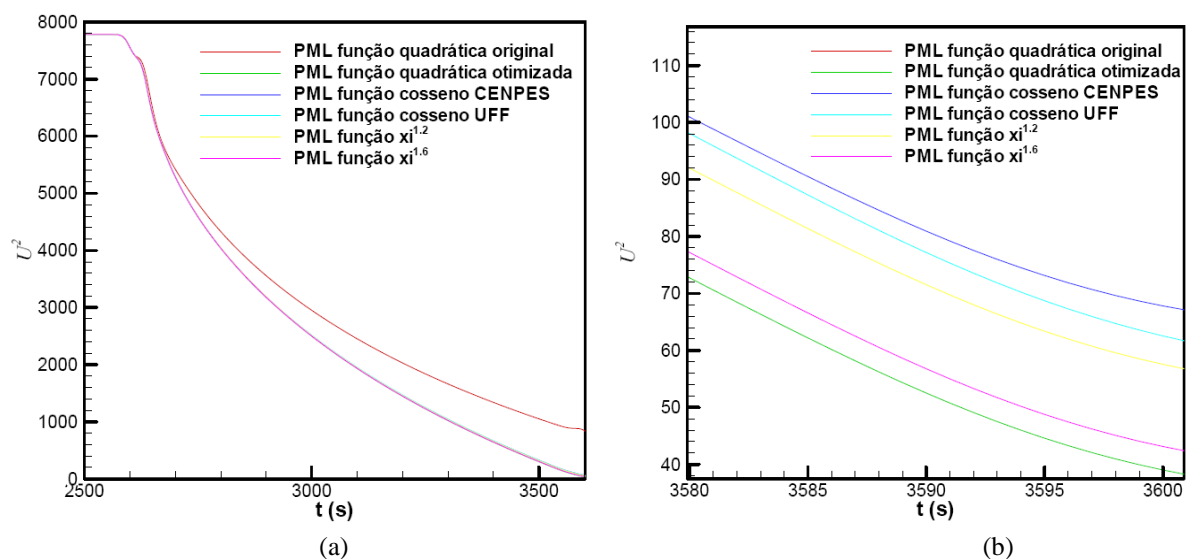


Figure 9. Optimized PML: total reflected energy for different attenuation functions  $f[x(i)]$ .

### 6.2 ABC and Hybrid Techniques

The ABC and DZ techniques have their results compared. In the first example in figure 10, a source with 5.64 Hz was used and the techniques of ABC, ABC + Liu, Cerjan Optimized with 20 layer points, and the combination ABC+Liu+Cerjan were applied. Notice that Cerjan had a worse performance compared to other techniques, which practically reduced to zero emission energy. In the following figure 10 one can see a detail and can be seen that the absorber ABC and ABC + Liu worked better than the combination with the Cerjan absorber.

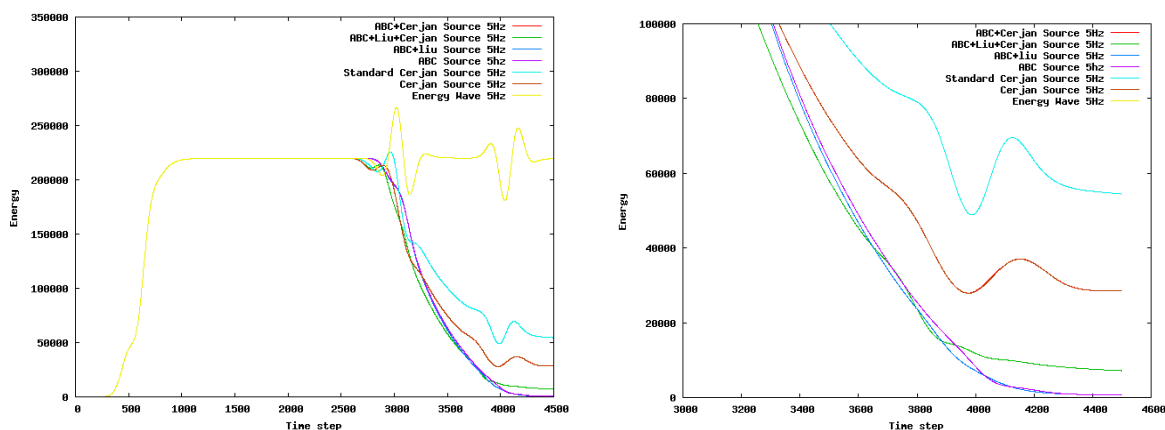


Figure 10 – Energy of the various absorbing methods with a source of 5Hz and a detail.

Table 1 shows the absorbing tax for the various methods. Notice that the ABC Method and the ABC+Liu works better than the DZ Methods. The results of PML and DZ can be improved using more points on the boundary layer.

Case 5Hz	Final Energy	Absorbing Tax
Without Absorber	219458	0%
ABC	618	99,72%
ABC+Liu	601	99,73%
Cerjan Standard	54434	75,19%
Dz Optimized	26271	88,02%
ABC+DZ	26272	88,02%
ABC+Liu+DZ	11070	94,96%
PML Optimized	72322	67,04%
ABC+PML	72301	67,05%
DZ+PML	37905	82,72%
ABC+DZ+PML	37909	82,72%
ABC+Liu+DZ+PML	31257	85,75%

Table 1 – Absorbing tax for a source of 5Hz

In a second example, the frequency was increased to 30Hz and results are shown on Figure 11. Note that the Cerjan Optimized improved considerably, but the absorption of ABC+Liu was better.

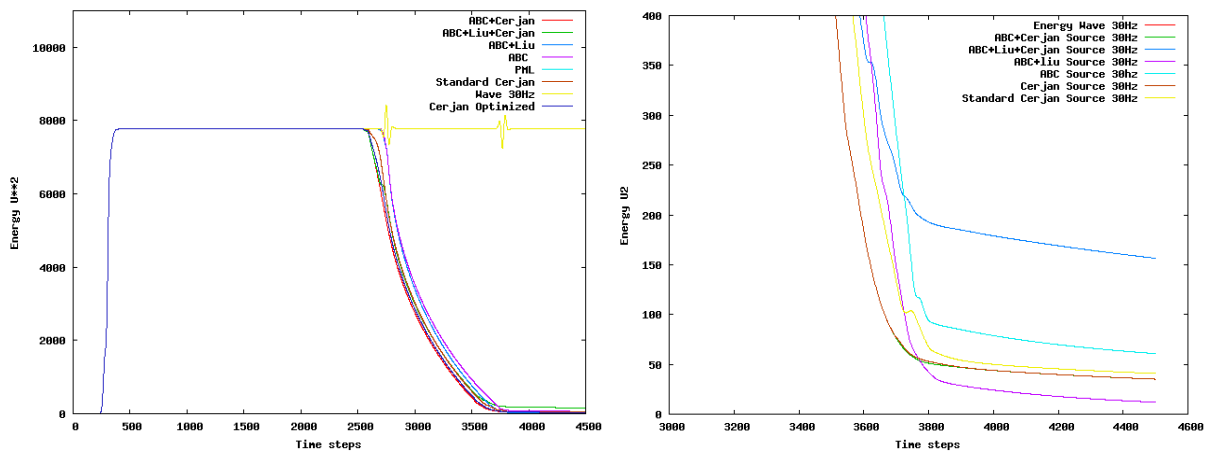


Figure 11 – Energy of the various absorbing methods with a source of 30Hz and a detail.

In table 2, one can see the absorbing tax. Notice that the results are much better. In fact, it can be seen that the efficiency varies with the frequency source. Specially Dz and PML Optimized Methods seen to be quite sensitive due to the frequency variation.

Case 30Hz	Final Energy	Absorbing Tax
<b>Without Absorber</b>	7782	0%
<b>ABC</b>	60,70	99,21%
<b>ABC+Liu</b>	11,96	99,84%
<b>Standard Cerjan</b>	40,81	99,48%
<b>DZ Optimized</b>	40,79	99,47%
<b>ABC+DZ Optimized</b>	40,76	99,47%
<b>ABC+Liu+Cerjan</b>	44,51	97,98%
<b>PML Optimized</b>	29,74	99,57%
<b>ABC+PML</b>	29,66	99,57%
<b>DZ+PML</b>	35,78	99,53%
<b>ABC+DZ+PML</b>	35,78	99,53%
<b>ABC+Liu+DZ+PML</b>	41,50	99,48%

Table 2 – Absorbing tax for a source of 30Hz

Finally in figure 12 we show the CPU time. Notice that the PML Optimized and ABC Method work faster and have a good absorbing tax. The incorporation of the Liu Method increases significantly the absorbing tax but also increase the CPU time. However, it is well known that the efficiency of the ABC methods depends on the wave incidence angle on the boundary surface. So, other tests with these types of problem have to be done in order to set a final conclusion. In this problem, the PML optimized was the best choice that conjugates good performance with low CPU tax.

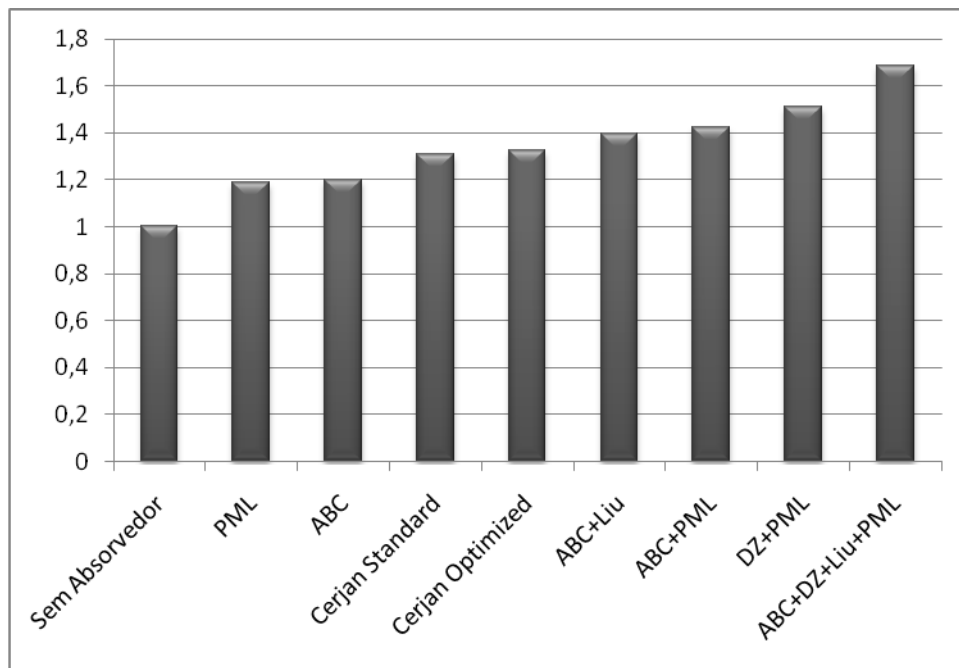


Figure 12 – CPU Time for the various methods

## 7 CONCLUSIONS

Some classical nonreflecting boundary methods – PML, DZ and ABC – were optimized aiming to reduce wave reflections at the borders of the FDTD 2D computational domain. It has been found that optimizations increase the effectiveness of the absorbing layer, with better absorption efficiencies for the ABC and optimized DZ and PML methods. Results also show that side effects are very sensitive to the source frequency and the number of grid points used in the absorbing layer, with better results found for larger discretization points. Hybrid alternatives are also tested. The corresponding absorbing factors are optimized again and results are presented in terms of the number of boundary layer points, CPU time and the total energy of the system.

## ACKNOWLEDGMENTS

The authors from UFF acknowledge the financial support through PETROBRAS.

## REFERENCES

- Berenger, J.-P. , A Perfectly Matched Layer for the Absorption of Electromagnetic Waves. *J. Comp. Phys.*, v.114, pp.185-200, 1994.
- Cerjan, C., Kosloff, D., Kosloff, R. and Reshef, M., A nonreflecting boundary condition for discrete acoustic and elastic wave equation. *Geophysics*, 50, 705-708, 1985.
- Clayton, R. and Engquist, B., Absorbing boundary conditions for acoustic and elastic wave equation. *Bull. Seis. Am.*, v.67, pp.1529-1540, 1977.
- Collino, F. and Tsogka, C., Application of the perfectly matched absorbing layer model to the linear elastodynamic problem in anisotropic heterogeneous media. *Geophysics*, v.66, pp.294–307. 2001.
- Durrant, D.R., *Numerical Methods for Wave Equations in Geophysical Fluid Dynamics*. New York: Springer-Verlag, 1999.
- Fan, G.-X. and Liu, Q.H., An FDTD Algorithm with Perfectly Matched Layers for General Dispersive Media. *IEEE Trans. On Antennas and Propagation*, v.48, no.5, pp.637-646, 2000.
- Liu, Y. and Sen, M.K., A hybrid scheme for absorbing edge reflections in numerical modeling of wave propagation, *Geophysics*, vol 75, 2010.
- Kreyszig, E., *Advanced Engineering Mathematics*. Singapore: John Wiley and Sons, 1993
- Marfurt K, Accuracy of finite-difference and finite-element modeling of the scalar and elastic wave equations. *Geophysics*, v.49, pp.533-549. 1984.
- Reynolds, A.C., Boundary conditions for the numerical solution of wave propagation problems. *Geophysics*, v.43, pp.1099-1110. 1978.
- Schuster, G.T., A hybrid BIE + Born series modeling scheme: General Born series. *Jour. of Acoustic Soc. of Am.*, v.77, pp.865-879, 1985.
- Sommerfeld, A., *Partial Differential Equations in Physics*. New York: Academic Press, 1949.
- Virieux, J., P-SV wave propagation in heterogeneous media: Velocity-stress finite-difference method. *Geophysics*, v.51, pp.889-901, 1986.
- Whitham, G.B., *Linear and Nonlinear Waves*. New York: John Wiley and Sons, 1999.